Influence of unloading modes of spring-mass-damper models on vehicle to pole collision simulation results

H.R. Karimi[1], W. Pawlus[1] and K.G. Robbersmyr[1]
1. Department of Engineering, Faculty of Engineering and Science, University of Agder, N-4898 Grimstad, Norway
E-mail: hamid.r.karimi@uia.no

Abstract:
Our intention, in this brief note, is to investigate what influence the viscoelastic models' unloading properties have on models' accuracy of representing vehicle crash event. Two types of simple spring-mass-damper systems (Kelvin models) such underdamped and critically damped conditions are analyzed. Subsequently, two different unloading scenarios are specified: elastic rebound in which only the damper is an energy dissipating element and plastic collision in which the model's maximum achievable displacement is at the same time its constant deflection at the zero-force level. By comparing models' behavior not only in terms of their time responses but also in terms of their force-deflection characteristics, it is concluded which of them is the most suitable to represent vehicle to pole collision.

Key Words: Model analysis, spring-mass-damper model, vehicle collision, simulation

1 INTRODUCTION

Vehicle users' safety is one of the great concerns of everyone who is involved in the automotive industry. However, crash tests are complex and complicated experiments. Therefore it is advisable to establish a vehicle crash model and use its results instead of a full-scale experiment measurements to predict car's behavior during a collision.

Nowadays we can distinguish two main approaches in this area. The first one utilizes FEM (Finite Element Method) software while the second way is called LPM (Lumped Parameter Modeling). There is a number of methods which can be applied to assess parameters of such models (stiffness, damping) basing on the real crash data. One of them is fitting the models' responses to the real car's displacement - see [1],[2], and [3].

Because of the fact that crash pulse is a complex signal, it is justified to simplify it. One solution for this is covered in [4]. References [5], [6], and [7] talk over commonly used ways of describing a collision e.g. investigation of tire marks or the crash energy approach.

Vehicle crash investigation is an area of up-to-date technologies application. References [8], [9], [10] and [11] discuss usefulness of such developments as neural networks or fuzzy logic in the field of modeling of crash events. Fuzzy logic together with neural networks and image processing have been employed in [12] to estimate the total deformation energy released during a collision.

In the most recent scope of research concerning crashworthiness it is to define a dynamic vehicle crash model which parameters will be changing according to the changeable input (e.g. initial impact velocity). One of such trials is presented in [13]. In addition to this work, in [14] one can find a complete derivation of vehicle collision mathematical models composed of springs, dampers and masses with piecewise nonlinear characteristics of springs and dampers.

The main contribution of this paper is the evaluation of the presented vehicle crash modeling methods with the full-scale experimental data elaborated in [15]. We prove that even the basic configuration of spring and damper (so called Kelvin model) is able to simulate a vehicle crash providing us with the satisfactory results. Application of two different types of responses of this system (underdamped and critically damped) as well as two different types of unloading characteristics (elastic and plastic) give us the full insight into the vehicle crash phenomena.

2 KELVIN MODEL

An arrangement in which a spring and a damper are connected in parallel to a mass is called Kelvin model - see Fig. 1.

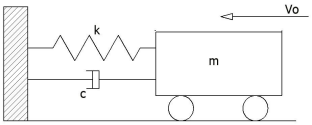

Fig. 1: Kelvin model

The following notation has been used: m - vehicle mass $[kg]$, k - spring stiffness $[N/m]$, c - damping coefficient $[Ns/m]$, v_0 - initial impact velocity $[m/s]$.

2.1 Underdamped system ($0 < \zeta < 1$)

Closed-form solutions for the transient responses of this system (displacement, velocity and acceleration, respectively) have the following form:

$$\alpha(t) = \frac{v_0 e^{-\zeta\omega t}}{\sqrt{1-\zeta^2}\omega} \sin\left(\sqrt{1-\zeta^2}\omega t\right) \tag{1}$$

$$\dot{\alpha}(t) = v_0 e^{-\zeta\omega t}\Big[\cos\left(\sqrt{1-\zeta^2}\omega t\right) - \frac{\zeta}{\sqrt{1-\zeta^2}} \sin\left(\sqrt{1-\zeta^2}\omega t\right)\Big] \tag{2}$$

$$\ddot{\alpha}(t) = v_0\omega e^{-\zeta\omega t}\Big[-2\zeta\cos\left(\sqrt{1-\zeta^2}\omega t\right) + \frac{2\zeta^2-1}{\sqrt{1-\zeta^2}} \sin\left(\sqrt{1-\zeta^2}\omega t\right)\Big] \tag{3}$$

where:

$\omega = \sqrt{\frac{k}{m}}$ - circular natural frequency $[rad/s]$

$\zeta = \frac{c}{2m\omega}$ - damping factor.

2.2 Critically damped system ($\zeta = 1$)

The transient responses of this system are as follows:

$$\alpha(t) = v_0 t e^{-\omega t} \tag{4}$$

$$\dot{\alpha}(t) = v_0(1 - \omega t)e^{-\omega t} \tag{5}$$

$$\ddot{\alpha}(t) = v_0\omega(\omega t - 2)e^{-\omega t}. \tag{6}$$

2.3 Energy absorption in the loading phase

When a vehicle hits an obstacle (e.g. a rigid barrier), it moves until the maximum crush is achieved - this stage is referred to so called loading phase - see [16]. In this phase, car's kinetic energy is consumed as its deformation and dissipated as the heat. Similarly for a spring and a damper - they absorb the model's initial kinetic energy (in the formulas below x is model's displacement):

$E_k = \frac{1}{2}kx^2$ - *energy absorption by the spring*

$E = \frac{1}{2}mv_0^2$ - *total kinetic energy*

$E_c = E - E_k$ - *energy absorption by the damper*.

2.4 Model parameters establishment from the real data

In order to establish model's parameters, it is desirable to rearrange (1) and (4) and express them only in terms of spring stiffness k and/or damping coefficient c:

underdamped system:

$$\alpha(t) = 2 \cdot \frac{v_0 e^{-\frac{ct}{2m}} \cdot \sin\left(\frac{1}{2}\sqrt{4 - \frac{c^2}{km}} \cdot \sqrt{\frac{k}{m}}t\right)}{\sqrt{4 - \frac{c^2}{km}} \cdot \sqrt{\frac{k}{m}}} \tag{7}$$

critically damped system:

$$\alpha(t) = v_0 t e^{-\sqrt{\frac{k}{m}}t} \tag{8}$$

where model's mass m and initial velocity v_0 are selected according to the experimental data. Now we can fit modified models' responses (7) and (8) to the real car's crush and as an outcome of this operation obtain the energy absorber's (EA) parameters (spring stiffnes k and damping coefficient c).

3 EXPERIMENTAL SETUP DESCRIPTION

The data used by us come from the typical vehicle to pole collision. The initial velocity of the car was 35 km/h, and the mass of the vehicle (together with the measuring equipment and dummy) was 873 kg. During the test, the acceleration at the center of gravity in three dimensions (x - longitudinal, y - lateral and z - vertical) was recorded. The yaw rate was also measured with a gyro meter. Using normal speed and high-speed video cameras, the behavior of the safety barrier and the test vehicle during the collision was recorded - see Fig. 2.

3.1 Test procedure

This vehicle to pole collision was performed at Lista Airport (Farsund, Norway) in 2004. A test vehicle was subjected to impact with a vertical, rigid cylinder. During the test, the acceleration was measured in three directions (longitudinal, lateral and vertical) together with the yaw rate from the center of gravity of the car. The acceleration field was 100 meter long and had two anchored parallel pipelines. The pipelines have a clearance of 5 mm to the front wheel tires. The force to accelerate the test vehicle was generated using a truck and a tackle. The release mechanism was placed 2 m before the end of the pipelines and the distance from there to the test item was 6.5 m. The vehicle was steered using the pipelines that were bolted to the concrete runaway. Experiment's scheme is shown in Fig. 3.

Fig. 2: Subsequent steps of crash test

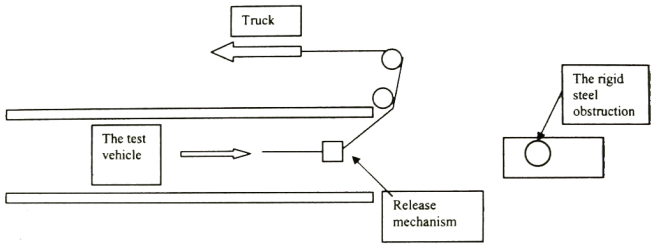

Fig. 3: *Scheme of the crash test [15].*

3.2 Description of the car and pole

The initial velocity of the car was 35 km/h, and the mass of the vehicle (together with the measuring equipment and dummy) was 873 kg. Particular car's parameters are illustrated in Fig. 4.

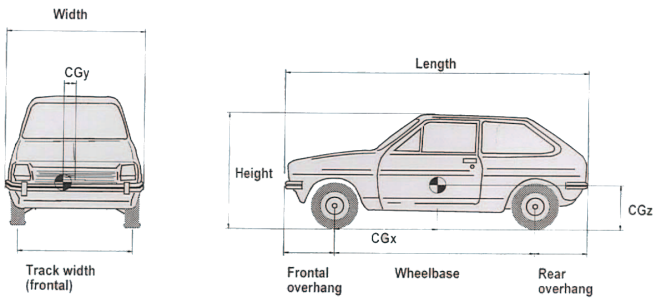

Fig. 4: *Car's dimensions [15].*

When it comes to the pole (obstruction), it was constructed with two components, a baseplate and a pipe. Both of them were made of steel. The baseplate had dimensions $740 \times 410 \times 25$ mm. The pipe had length 1290 mm and overall diameter equal to 275 mm. The obstruction pipe was filled with concrete and mounted on a concrete foundation with 5 bolts. These bolts connected the concrete foundation and the baseplate of the obstruction which was fixed to shovel of a heavy machine.

3.3 Instrumentation

As it has been already mentioned, during the test, the acceleration at the center of gravity in three dimensions (x - longitudinal, y - lateral and z - vertical) was recorded. The vehicle speed before the collision was measured. The yaw rate was also measured with a gyro meter. Using normal speed and high - speed video cameras, the behaviour of the safety barrier and the test vehicle during the collision was recorded - video recorders' arrangement is presented in Fig. 5.

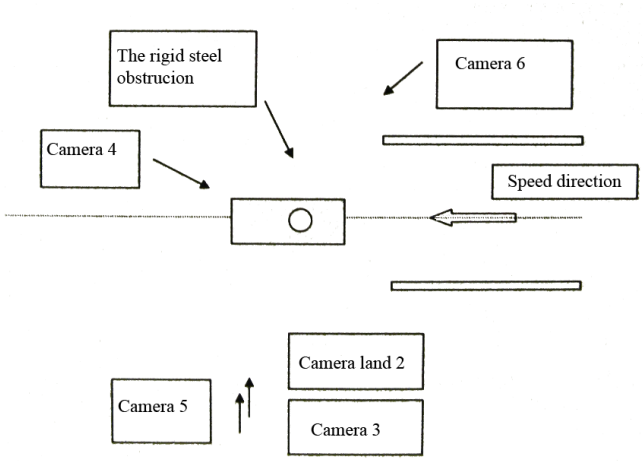

Fig. 5: *Layout of the cameras in the crash test [15].*

Using two 3 - D accelerometers the acceleration was recorded. The accelerometer was a piezoresistive triaxial sensor with a range of plus - minus 1500 g. Those devices were mounted on a steel bracket close to the vehicle's center of gravity and the bracket was fastened by screws to the vehicle's chassis. The yaw rate was measured with a gyro instrument which makes it is possible to record $1^{\circ}/sec$. Data from the sensors was fed to an eight channel data logger and subsequently sampled with a frequency of 10 kHz. The memory was able to store 6.5 sec of data per channel. The velocity of the vehicle was checked by an inductive monitor. It was directed towards a perforated disc mounted on a wheel on the right side of the test vehicle. Fig. 6 shows the car before, during and after the collision.

Remark 1. It is noting that the data acquisition process has to be carried out correctly - e.g. accuracy of determination of the car's center of gravity plays an important role because accelerometer is placed close to that point. Furthermore, the measurement itself has the great influence on the subsequent signals' analysis - parameters such as sampling rate or recording's duration should be selected appropriately. Therefore it is justified to propose a mathematical model which could be used instead of such a costly experiment and which could give the results similar to the real car's behavior.

3.4 Crash pulse analysis

Having at our disposal the acceleration measurements from the collision, we are able to describe in details motion of the car. Since it is a central impact, we analyze only the pulse recorded in the longitudinal direction (x-axis). By integrating car's deceleration we obtain plots of velocity and displacement, respectively - see Fig. 7. At the time t_m when

Fig. 6: *Car's deformation [15].*

the relative approach velocity is zero, the maximum dynamic crush C occurs.

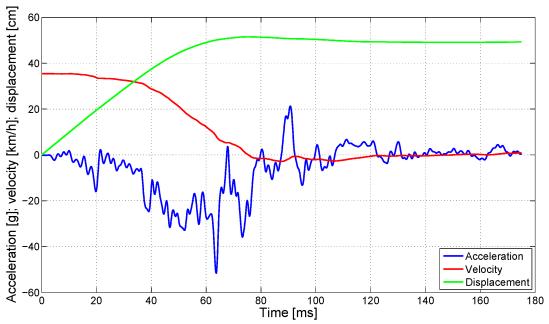

Fig. 7: Car's kinematics

4 MODELS ESTABLISHMENT

For the simulation purposes, the unloading stiffness k_u is assumed to be infinitely large. The initial impact velocity is the same as the one in the crash test ($v_0 = 9.86\ m/s$) - this also holds when it comes to the model's mass ($m = 873\ kg$).

According to the method decribed in section 2.4 (fitting has been performed in MATLAB software), loading spring stiffness and damping coefficient for underdamped and critically damped system are determined to be $k = 112660\ N/m$, $c = 7446\ N/m$ and $k = 42290\ N/m$,

$c = 12152\ N/m$, respectively. Comparative analyses between force-deflection characteristics of two types of unloading scenarios and between models' and car's displacements are shown in Fig. 8 and Fig. 9, respectively.

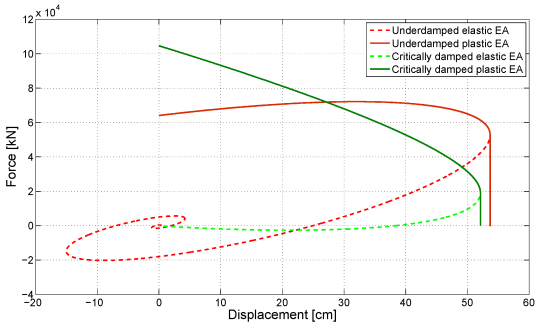

Fig. 8: Force-deflection curves

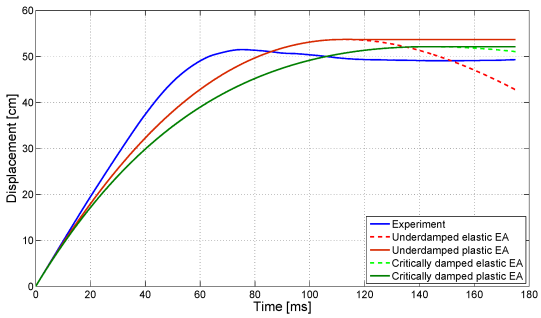

Fig. 9: Time responses comparison

It is noting that in Fig. 8 the elastic energy absorbers reach the zero-force level, even though it is not shown in Fig. 9. That is because the time responses comparison has been done only in the crush time interval ($0.175\ ms$) to better visualize models' fidelity. Table 1 presents comparison between particular car's and models' crash parameters.

Table 1: Relevant parameters characterizing collision

Parameter	Underdamped	Critically damped	Experiment
$C\ [cm]$	54	52	51
$t_m\ [cm]$	113	144	76
$E\ [kJ]$	42.44	42.44	42.44
$E_k\ [kJ]$	16.43	5.72	-
$E_c\ [kJ]$	26.01	36.72	-

5 CONCLUSIONS AND FUTURE WORKS

5.1 Conclusions

Extending a simple linear spring-mass-damper model to the one which exhibits plastic unloading properties has improved the accuracy of models' simulation results. Since a vehicle to pole collision is a type of crash event in which a lot of energy is dissipated (it's a localized impact therefore the rebound is relatively small - from Fig. 9 we see that for the full-scale crash test which we deal with the elastic displacement is equal to 2 cm), it is advisable to represent it by a model which displacement in the unloading phase (i.e. after the rebound) is also small or even negligible. This has been achieved by employing a plastic spring-mass-damper model - results confirmed that both systems with plastic unloading scenarios (underdamped and critically damped) approximate the real car's crush quite well. However, the best overall performance has been achieved for the underdamped Kelvin model, since the maximum dynamic crush has been reached quite faster than in the case of critically damped system.

5.2 Future Works

Method presented by us is simple and gives reasonable results. However, to represent in details car's bahavior, it is advisable to extend the simple spring-mass-damper model to the more complex one. For that reason in the future work we will investigate hybrid models (arrangements composed of several springs, dampers and masses in various configurations). What is more, the results may also be improved by establishing a couple of unloading stiffnesses, making it possible to simulate the rebound of the system more accurately. Apart from that, applying springs and dampers with nonlinear characteristics (since most of the real world materials exhibit nonlinear force-deflection performance) will let us increase models' fidelity.

References

[1] W. Pawlus, J.E. Nielsen, H.R. Karimi, and K.G. Robbersmyr, Mathematical modeling and analysis of a vehicle crash, *The 4th European Computing Conference*, Bucharest, Romania, April 2010.

[2] W. Pawlus, J.E. Nielsen, H.R. Karimi, and K.G. Robbersmyr, Development of mathematical models for analysis of a vehicle crash, *WSEAS Transactions on Applied and Theoretical Mechanics*, vol.5, no.2, pp.156-165, 2010.

[3] W. Pawlus, J.E. Nielsen, H.R. Karimi, and K.G. Robbersmyr, Further results on mathematical models of vehicle localized impact, *The 3rd International Symposium on Systems and Control in Aeronautics and Astronautics*, Harbin, China, June 2010.

[4] H.R. Karimi and K.G. Robbersmyr, Wavelet-based signal analysis of a vehicle crash test with a fixed safety barrier, *WSEAS 4th European Computing Conference*, Bucharest, Romania, April 20-22, 2010.

[5] G. Šušteršič, I. Grabec, and I. Prebil, Statistical model of a vehicle-to-barrier collision, *International Journal of Impact Engineering*, vol.34, no.10, pp.1585-1593, 2007.

[6] D. Trusca, A. Soica, B. Benea, and S. Tarulescu, Computer simulation and experimental research of the vehicle impact, *WSEAS Transactions on Computers*, vol.8, no.1, pp.1185 - 1194, 2009.

[7] D. Vangi, Energy loss in vehicle to vehicle oblique impact, *International Journal of Impact Engineering*, vol.36, no.3, pp.512-521, 2009.

[8] V. Giavotto, L. Puccinelli, M. Borri, A. Edelman, and T. Heijer, Vehicle dynamics and crash dynamics with minicomputer, *Computers and Structures*, vol.16 no1, pp.381-393, 1983.

[9] I.A. Harmati, A. Rovid, L. Szeidl, and P. Varlaki, Energy distribution modeling of car body deformation using LPV representations and fuzzy reasoning, *WSEAS Transactions on Systems*, vol.7, no.1, pp.1228-1237, 2008.

[10] T. Omar, A. Eskandarian, and N. Bedewi, Vehicle crash modelling using recurrent neural networks, *Mathematical and Computer Modelling*, vol.28, no.9, pp.31-42, 1998.

[11] W. Pawlus, J.E. Nielsen, H.R. Karimi, and K.G. Robbersmyr,

Comparative analysis of vehicle to pole collision models established using analytical methods and neural networks, *The 5th IET International System Safety Conference*, Manchester, UK, October 2010.

[12] A.R. Várkonyi-Kóczy, A. R¨ovid, P. Várlaki. Intelligent methods for car deformation modeling and crash speed estimation, *The 1st Romanian-Hungarian Joint Symposium on Applied Computational Intelligence*, Timisoara, Romania, May 2004.

[13] E. van der Laan, F. Veldpaus, B. de Jager, and M. Steinbuch, LPV modeling of vehicle occupants, *AVEC '08 9th International Symposium on Advanced Vehicle Control*, Kobe, Japan, October 2008.

[14] A.M. Elmarakbi and J.W. Zu, Crash analysis and modeling of two vehicles in frontal collisions using two types of smart front-end structures: an analytical approach using IHBM, *International Journal of Crashworhiness*, vol.11, no.5, pp.467-483, 2006.

[15] K.G. Robbersmyr, Calibration test of a standard ford fiesta 1.1l, model year 1987, according to NS - EN 12767, Technical Report 43/2004, Agder Research, Grimstad, 2004.

[16] M. Huang, Vehicle Crash Mechanics, CRC Press, Boca Raton, 2002.